Front. Earth Sci. 2022, 16(4): 963–974
https://doi.org/10.1007/s11707-022-0983-4

RESEARCH ARTICLE

Laboratory investigation of coal sample permeability under the coupled effect of temperature and stress

Yina YU[1], Zhaoping MENG (✉)[1,2], Jiangjiang LI[3], Yixin LU[1], Caixia GAO[3]

1 College of Geosciences and Surveying Engineering, China University of Mining and Technology (Beijing), Beijing 100083, China
2 State Key Laboratory of Coal and CBM Co-mining, Jincheng 048000, China
3 Exploration and Development Research Institute, PetroChina Huabei Oilfield Company, Renqiu 062552, China

Abstract The stress and temperature sensitivities of coal reservoirs are critical geological factors affecting coalbed methane (CBM) well exploitation; in particular it is important to reduce or eliminate their influence on coal reservoir permeability. To investigate coal permeability behavior at various effective stresses and temperatures, CH_4 permeability tests were conducted on raw coal samples under a varying effective stress of 2.0–8.0 MPa under five different temperatures (25°C–65°C) in the laboratory. The results show that the permeability of the coal samples exponentially decreases with increasing effective stress or temperature, which indicates obvious stress and temperature sensitivity. Through a dimensionless treatment of coal permeability, effective stress, and temperature, a new stress sensitivity index S and temperature index S_T are proposed to evaluate coal stress and temperature sensitivity evaluation parameters. These new parameters exhibit integrality and uniqueness, and, in combination with stress sensitivity coefficient α_k, temperature sensitivity coefficient α_T, and the permeability damage rate *PDR*, the sensitivities of coal permeability to stress and temperature are evaluated. The results indicate that coal sample stress sensitivity decreases with increasing effective stress, while it first decreases and then increases with increasing temperature. Additionally, coal sample temperature sensitivity shows a downward trend when temperature increases and fluctuates when effective stress increases. Finally, a coupled coal permeability model considering the impacts of effective stress and temperature is established, and the main factors affecting coal reservoir permeability and their control mechanism are explored. These results can provide some theoretical guidance for the further development of deep CBM.

Keywords deep coal reservoir, permeability variation, stress sensitivity, temperature sensitivity

Received November 30, 2021; accepted March 17, 2022

E-mail: mzp@cumtb.edu.cn

1 Introduction

Coal reservoirs, as well as the stored and transported coalbed methane (CBM) produced therein, are subjected to a variety of energy fields, such as *in situ* stress fields, groundwater pressure fields, and geothermal fields. Changes in the conditions of these energy fields, such as the stress, pressure, and temperature of coal reservoirs, lead to transformations between gas adsorption and desorption, with a significant influence on CBM production. Therefore, to efficiently exploit CBM resources, it is important to explore dynamic changes to coal permeability under the coupled effect of temperature and stress.

Research on coal reservoir permeability under temperature and stress-coupled actions began with Terzaghi's study of land subsidence. Terzaghi (1943) proposed a formula for calculating effective stress and established a one-dimensional consolidation model that remains one of the basic methods for studying the interaction between rock and fluid. Based on Terzaghi's work, Biot (1954) extended the one-dimensional consolidation model to a three-dimensional, elastic consolidation analysis. Since the 1980s, a series of investigations based on seepage theory and both physical and numerical simulations of multifield coupling in porous media have been carried out, and governing equations have been established for the relevant solid mechanics, fluid seepage, and thermal fields (Ohnishi et al., 1982; Oda, 1985; Norishad, 1989; Pan and Connell, 2012; Liu and Liu, 2014; Liu et al., 2017; Gao et al., 2021). For example, Liu et al. (2017) considered the interaction between coal and CBM, establishing a mathematical model of solid–gas coupling that was able to reveal the migration law of coalbed gas. Gao et al. (2021) considered the impact of temperature on coal matrix adsorption deformation, improving the

seepage model of coupling among stress fields, flow fields, and temperature fields; thus, the coupling model can be used to represent CBM migration under the action of multiple fields.

Coal reservoirs represent a type of dual-porosity medium with a special pore-fracture structure, which makes coal reservoir permeability change more significantly with stress than conventional oil and gas reservoirs. Somerton et al. (1975) were the first to establish a coal permeability calculation equation for a system under effective stress. On this basis, Durucan and Edwards (1986) carried out seepage experiments, believing that with rising effective stress, coal permeability would exponentially decline. Meng and Li (2013) conducted laboratory tests to characterize coal permeability variation under different stresses, in which they analyzed the effects of fractures, maceral content, and moisture on coal reservoir permeability.

At first, determinations of the impact of stress on coal reservoir permeability were mostly based on experimental research. With the development of CBM wells, abundant data from field production have been introduced. Sparks et al. (1995) studied the relationship between coal reservoir permeability and in situ stress using field-scale measurements for the first time. McKee et al. (1998) obtained permeability variation with burial depth data of coal reservoirs in the Black Warrio, San Juan, and Piceance Basins, finding that with increasing depth, coal pores and fracture apertures decreased, and permeability decreased exponentially. Meng et al. (2014), taking the Southern Qinshui Basin as a research subject, analyzed CBM well test data from coal reservoirs, proposed a prediction model of geo-stress and pore pressure, and established a function to describe reservoir permeability variation with geo-stress. In addition, computational models have been proposed to quantitatively determine the impact of stress on coal reservoir permeability (Shi and Durucan, 2005; Meng et al., 2018; Karthikeyan et al., 2020) and thereby theoretically explain the phenomena observed in the field and in experiments.

Temperature is another crucial factor influencing CBM seepage flow. There have been many studies of the relationship between coal permeability and temperature, with remarkable progress being achieved. It has been found that coal permeability generally decreases with increasing temperature under a given effective stress condition (Bear and Corapcioglu, 1981; Yin et al., 2013; Chu et al., 2016; Wang et al., 2019). Perera (2017) proposed that the influence of temperature on permeability is dependent on effective stress degree; conversely, the effect of temperature on permeability is different under different stress states. An increase in temperature would induce coal matrix expansion deformation, with an expanding coal matrix squeezing CBM seepage channels and thereby reducing coal permeability (Li et al., 2009). Moreover, an increase in temperature will promote the desorption of CBM, inducing coal matrix shrinkage and subsequently increasing coal permeability (Sakurovs et al., 2008). As temperature increases further, at a certain value, the weakest parts of the coal matrix will reach a critical state and become activation sites, developing into new cracks (Akbarzadeh and Chalaturnyk, 2014), which increases the number of CBM seepage flow channels and results in a sharp increase in coal reservoir permeability. Combined with previous research results, coal permeability evolution with temperature can be summarized by a U-shaped curve with four stages: rapid decline, stabilization, slow rise, and sharp rise (Teng et al., 2016; Shang et al., 2019). These correspond to four effects, respectively: thermal expansion, desorption-induced matrix shrinkage, thermal cracking, and fracture penetration.

However, previous studies have not sufficiently considered stress and temperature coupling impacts on coal reservoir permeability, which has resulted in a poor understanding of how to control drainage in CBM wells. Therefore, in this paper, based on geo-stress and geothermal field conditions in the Qinshui Basin, a triaxial seepage test system is used to simulate and analyze the seepage law and control mechanism of methane in coal at different effective stresses and temperatures. The permeability damage rate (*PDR*), stress sensitivity coefficient α_k, temperature sensitivity coefficient α_T, and a new stress sensitivity index S and temperature index S_T have been introduced to quantitatively evaluate the variation law of permeability in CBM production under different temperatures. Finally, a coupling control model of temperature and effective stress on medium-rank coal permeability is established, which would provide theoretical guidance for CBM development in deep coal reservoirs.

2 Experimental conditions and procedures

Each coal sample for the seepage experiment was cylindrical with a length and diameter of 50 mm and 25 mm, respectively, sampled from coal reservoir No. 3 at the Changzhi Coal Mine, Qinshui Basin, Shanxi, China. The coal reservoir average thickness of coal reservoir No. 3 was 5.71 m, distributed in thin strips in the lower part of the Permian Shanxi Formation with a glassy luster. The coal lithotype belonged mainly to bright coal, followed by vitrinite (Meng and Liu, 2018). The maximum vitrinite reflectance (R_o) of the coal samples was 1.71%, in the low-volatile bituminous coal range. According to an approximate analysis on an air-dried basis, the moisture content (M_{ad}), ash yield (A_{ad}), and volatile matter content (V_{ad}) of the samples were 1.22%, 10.99%, and 11.53%, respectively.

As mentioned, the occurrence and production of CBM are controlled by multiple fields, including *in situ* stress, groundwater pressure, as well as geothermal fields (Fig. 1).

To analyze coal reservoir permeability evolution under geothermal field and effective stress coupled effects, we simulate the environmental conditions of the reservoir using different axial pressures, confining pressures, and temperatures, and measure the variations in the coal permeability. Table 1 provides the experimental temperature and stress conditions.

As shown in Fig. 2, the experimental apparatus is an improved CBM seepage simulation apparatus (CBM-DR-1A); its principal parts include a high-pressure advection pump, a triaxial core holder, two thermostats, inlet and outlet pressure regulators, flowmeters, a data processing system, and other auxiliary equipment. Coal permeability evolution under different *in situ* stresses, reservoir pressures, and temperatures could be simulated by adjusting the axial and confining pressure, temperature, and inlet and outlet gas pressures.

To ensure stability throughout the experimental procedure, it was necessary to continuously monitor the gas pressure, axial pressure, confining pressure, and temperature. The experiment process was as follows.

1) Before the seepage experiment, the air-tightness of the seepage apparatus was checked, and vacuum degassing was conducted for 12 h.

2) During the seepage experiment, the axial and confining pressures were provided by injecting water into the core holder via constant-pressure pumps. To prevent shear failure of the sample, the experimental axial pressure was kept higher than experimental confining pressure. The temperatures of the experimental fluid and coal sample were controlled through the thermostats outside the gas holder and core holder.

3) The axial pressure, confining pressure, and the first temperature point (25°C) were alternately loaded to the desired values and maintained for at least 12 h to ensure that the coal sample deformation reached a new equilibrium state.

4) The test gas (CH_4) was injected at a constant pressure; importantly, the state should be maintained for more than 12 h once the pore pressure reached a predetermined value to ensure adsorption equilibrium of the coal sample.

5) The effective stress was kept unchanged and temperature test condition was changed to 35°C, 45°C, 55°C, and 65°C. It was also important that, under each new temperature test condition, the new temperature was held constant for at least 3 h to ensure that the coal sample achieved a new balance. After stable seepage appeared, the gas flow was recorded.

6) The permeability was tested by a steady-state method, and steps (2)–(5) were repeated so that, in all, seepage tests were carried out at effective stress of 2.0, 4.0, 6.0, and 8.0 MPa.

Coal sample gas permeability k_g (in units of $10^{-3}\cdot\mu m^2$) is calculated using Darcy's law as follows:

$$k_g = \frac{2P_0Q_gL\mu_g}{A\left(P_1^2 - P_2^2\right)}, \tag{1}$$

where P_0 (MPa) is the standard atmospheric pressure; Q_g (mL/s) is the flow of experimental fluid under P_0; P_1 (MPa) and P_2 (MPa) are the inlet and outlet gas pressure, respectively; A (cm^2) is the cross-sectional area of the coal sample; L (cm) is the height of the coal sample; μ_g (μPa·s) is the dynamic viscosity coefficient; μ_g is a temperature-dependent parameter. For CH_4, it can be calculated as follows (Li et al., 2009):

$$\mu_g = 1.36\times10^{-4}T^{0.77}, \tag{2}$$

where T (K) is the absolute temperature.

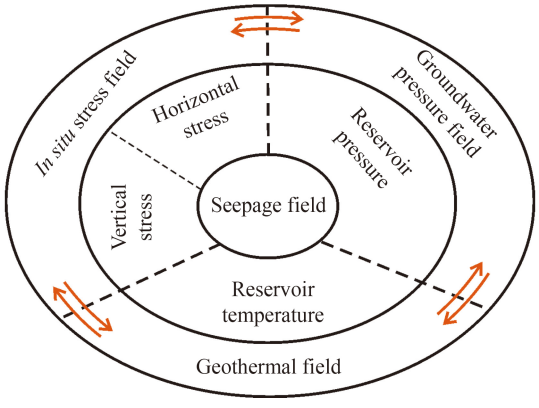

Fig. 1 Schematic of coal reservoir seepage field under multifield coupling.

Table 1 Specific temperatures and stress conditions for seepage experiments

Sample ID	Confining stress/MPa	Axial stress/MPa	Effective stress/MPa	Temperature/°C
S1	2.0	2.6	2.0	25/35/45/55/65
S2	4.0	4.6	4.0	25/35/45/55/65
S3	6.0	6.6	6.0	25/35/45/55/65
S4	8.0	8.6	8.0	25/35/45/55/65

Note: Effective stress = [(Confining pressure × 2 + Axial pressure)/3] − pore pressure.

3 Results and analysis

3.1 Permeability variation with effective stress at different temperatures

The effective stress impact on coal sample permeability under different temperatures is illustrated in Fig. 3(a). At 25 °C, coal permeability decreased from 0.310 × 10^{-3} to 0.09 × 10^{-3} μm^2 when the effective stress increased from 2.0 to 4.0 MPa, respectively. Coal sample permeability further decreased to 0.013 × 10^{-3} μm^2 when the effective stress increased to 8.0 MPa. The permeability variation at

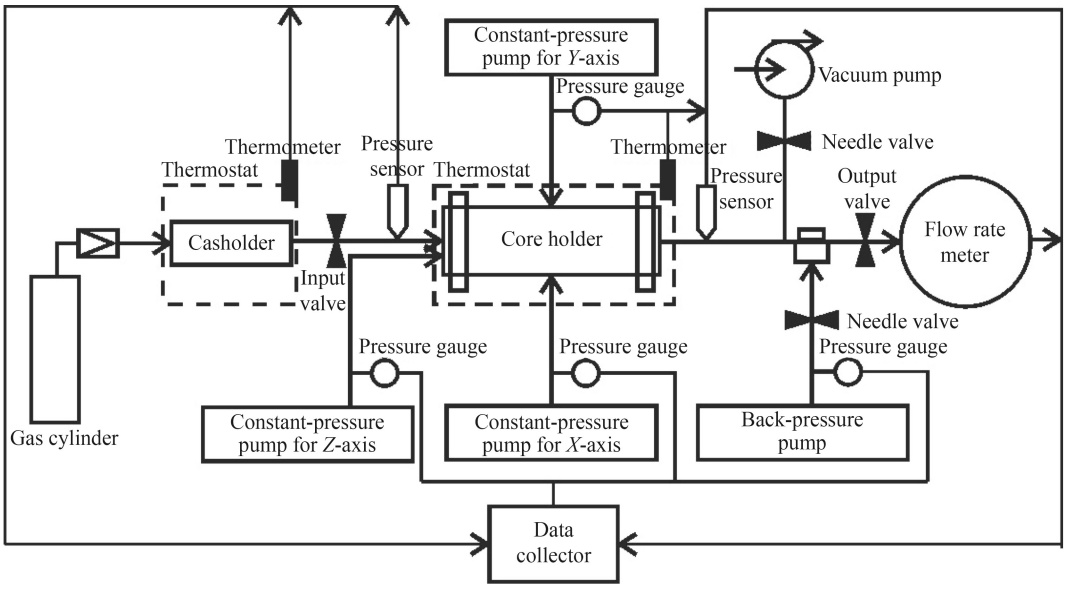

Fig. 2 Schematic of the experimental apparatus.

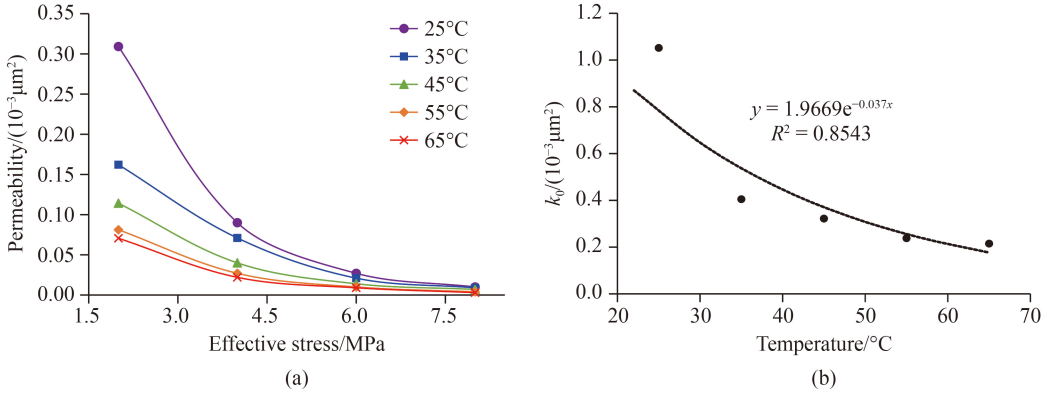

Fig. 3 (a) Coal permeability evolution with effective stress at different temperatures. (b) Initial coal permeability evolution with temperature.

the other experimental temperatures resembled that at 25°C. These results reveal that the permeability decreased sharply in the low-stress stage. With further increases in stress, the decrease in permeability gradually slowed down. Coal permeability curves corresponding to different temperatures exhibited obvious differences when the effective stress was low. With increasing effective stress, these differences became less. As effective stress increased above 6.0 MPa, the permeability curves under different temperatures almost coincided with each other.

Through a regression analysis of the experimental results, coal permeability evolution with effective stress at different temperatures can be represented by the following negative exponential form:

$$k_g = k_0 \exp(-a_1 \sigma_e), \quad (3)$$

where k_g ($10^{-3}\cdot\mu m^2$) is the gas permeability, σ_e (MPa) is the effective stress, k_0 ($10^{-3}\cdot\mu m^2$) is the permeability under the initial effective stress (0 MPa), and a_1 (MPa^{-1}) is the stress sensitivity regression coefficient.

The regression analysis results for coal sample permeability and effective stresses are represented in Table 2. The range of k_0 is 0.215×10^{-3}–1.052×10^{-3} μm², with a mean of 0.446×10^{-3} μm², showing a decreasing trend with increasing temperature (Fig. 3(b)). Additionally, a_1 ranges from 0.455 to 0.613 MPa^{-1}, with a mean of 0.536 MPa^{-1}, decreasing first and then increasing with rising temperature.

3.2 Permeability variation with temperature at different effective stresses

Coal reservoirs are always subjected to a certain temperature field. To explore the impact of temperature on coal reservoir permeability, stress sensitivity experiments were conducted at different temperatures, and coal sample permeability evolution with temperature under various stresses was analyzed.

Table 2 Regression coefficients between coal sample permeability and effective stress at different temperatures.

Temperature/°C	k_0/(10^{-3} μm^2)	a_1/(MPa^{-1})	R^2
25	1.052	0.613	0.999
35	0.405	0.455	0.999
45	0.322	0.518	0.996
55	0.238	0.538	0.999
65	0.215	0.557	0.999
Average	0.446	0.536	0.998
Maximum value	1.052	0.613	0.999
Minimum value	0.215	0.455	0.996

According to Fig. 4(a), coal sample permeability decreased with increasing temperature within the experimental range. A sharp decline was particularly obvious when at low temperatures. With a further increase in temperature, the overall trend in permeability was more moderate. In addition, the permeability curves corresponding to different effective stresses exhibited obvious differences when the temperature was low, but these differences became less significant with increasing temperature.

Under different effective stresses, the relation between coal sample permeability and temperature basically takes the following negative exponential form:

$$k_g = k_{0t}\exp(-a_2 T), \tag{4}$$

where k_g ($10^{-3}\cdot$μm^2) is the gas permeability, k_{0t} (10^{-3} μm^2) is the permeability at the initial temperature, the initial temperature is set to 0°C for convenience, a_2 (°C^{-1}) is the temperature sensitivity regression coefficient, and T (°C) is the coal temperature. Eq. (4) is applied to the data from seepage experiments under varying temperatures at various effective stresses, showing a good fit with the measured permeability data (>96%). The fitting result indicates that coal permeability would exponentially decrease with increasing temperature when the pore pressure is constant. According to Table 3, the range of k_{0t} is 0.034 × 10^{-3}–0.934 × 10^{-3} μm^2, with a mean of 0.393 × 10^{-3} μm^2, and k_{0t} decreases as a negative exponential function with increasing effective stress (Fig. 4(b)). In addition, a_2 ranges from 0.029°C^{-1} to 0.066°C^{-1}, with an average of 0.045°C^{-1}; with increasing effective stress, it first increases, then decreases, and then increases again.

4 Discussion

4.1 Evaluation parameters of stress and temperature sensitivity

In this study, to quantify the impact degree of effective stress and temperature on coal sample permeability, the industry standard No. SY/T5336, 5358, 6385 is referenced. The permeability damage rate *PDR*, stress sensitivity coefficient α_k, temperature sensitivity coefficient α_T, stress sensitivity index S, and temperature sensitivity index S_T are introduced to evaluate coal permeability stress sensitivity and temperature sensitivity.

1) The *PDR*: the *PDR* caused by stress or temperature sensitivity is defined as follows:

$$PDR = \frac{k_1 - k_i}{k_1} \times 100\%, \tag{5}$$

where k_i (10^{-3} μm^2) is the measured permeability after changing the stress or temperature conditions, and k_1 (10^{-3} μm^2) is the permeability at the initial temperature or stress point.

2) The α_k: the sensitivity coefficient of permeability to effective stress is defined as follows:

$$\alpha_k = -\frac{1}{k_0}\frac{\Delta k_g}{\Delta \sigma_e}, \tag{6}$$

where k_0 (10^{-3} μm^2) is the coal sample permeability at the initial stress, Δk_g (10^{-3} μm^2) is the change in coal sample permeability, and $\Delta\sigma_e$ (MPa) is the change in effective stress. From Eq. (6), at greater α_k values, coal

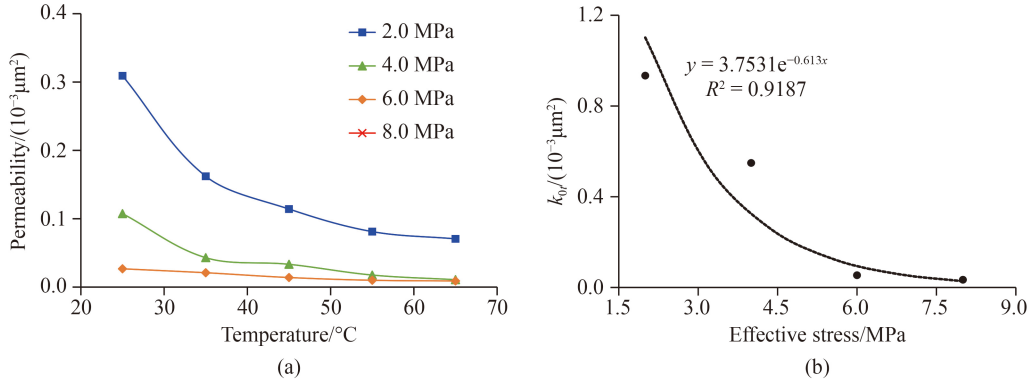

Fig. 4 (a) Coal permeability evolution with temperature at various effective stresses. (b) Initial coal permeability evolution with effective stress.

Table 3 Regression coefficients between coal sample permeability and temperature at different effective stresses.

Effective stress/MPa	k_{0t}/(10^{-3} μm^2)	a_2/(°C^{-1})	R^2
2.0	0.934	0.046	0.96
4.0	0.549	0.066	0.97
6.0	0.054	0.029	0.98
8.0	0.034	0.037	0.99
Avg.	0.393	0.045	0.98
Max. value	0.934	0.066	0.99
Min. value	0.034	0.029	0.96

permeability shows more sensitivity to changes in effective stress, that is, for a similar range of change in effective stress, coal sample permeability will be changed more. Conversely, at smaller α_k values, coal permeability shows weaker sensitivity to changes in effective stress, where under similar stress changes, coal sample permeability would change less.

3) A new stress sensitivity index S: based on a number of previous studies on stress sensitivity in oil and gas reservoirs, the following stress sensitivity coefficient has been proposed (Jones and Owens, 1980):

$$S = \frac{1-\left(\frac{K}{K_{1000}}\right)^{\frac{1}{3}}}{\log\frac{p_K}{1000}}, \tag{7}$$

where S is the dimensionless stress sensitivity coefficient, K (10^{-3} μm^2) is the coal permeability at net confining pressure p_K, and K_{1000} (10^{-3} μm^2) is the coal permeability at a net confining pressure of 1000 psi. As seen in Eq. (7), the stress sensitivity evaluation method must set a fixed net confining pressure value (1000 psi, approximately 7 MPa), which is difficult to control in experiments. If a fitting method is used to obtain the permeability at a net confining pressure of 1000 psi, this will lead to a loss of accuracy. Therefore, this paper introduces a new stress sensitivity index to assess coal sample permeability stress sensitivity by improving Eq. (7). The stress sensitivity index S is defined as follows:

$$S = -\log\left(\frac{k}{k_0}\right)/\log\left(\frac{\sigma}{\sigma_0}\right), \tag{8}$$

where k_0 (10^{-3} μm^2) and k (10^{-3} μm^2) are the coal sample permeabilities under the initial stress σ_0 and stress σ, respectively. Thus, S is obtained by putting the coal permeability and effective stress into dimensionless forms and taking their logarithms to base 10. The results are fitted, and the slope of the resulting line is S.

The stress sensitivity index S exhibits both integrality and uniqueness. First, the total number measured permeability and effective stress points have meet the statistical requirements of data processing, so the fitting results would provide an accurate reflection of coal sample stress sensitivity. Second, the stress sensitivity index S has the advantage as an evaluation parameter that its value is not affected by the number of measurement points or by temperature and stress conditions. Each given experimental condition corresponds to a unique value of S.

4) The α_T: the sensitivity coefficient of permeability to temperature is defined as follows:

$$\alpha_T = -\frac{1}{k_{0t}}\frac{\Delta k_g}{\Delta T}, \tag{9}$$

where k_{0t} (10^{-3} μm^2) is the coal sample permeability at the initial temperature, Δk_g (10^{-3} μm^2) is the change in coal sample permeability, and ΔT (°C) is the change in temperature.

5) A new temperature sensitivity index S_T: similar to Eq. (8), a new temperature sensitivity index S_T is proposed as an evaluation parameter for temperature influence on coal permeability, which is defined as follows:

$$S_T = -\log\left(\frac{k}{k_{0t}}\right)/\log\left(\frac{T}{T_0}\right), \tag{10}$$

where k_{0t} (10^{-3} μm^2) is the coal sample permeability at the initial temperature T_0, and k (10^{-3} μm^2) is the coal permeability at temperature T. The use of S_T avoids the influences of the initial value of the temperature and the number of permeability measuring points.

4.2 Evaluation of stress and temperature sensitivity of coal samples

4.2.1 Analysis of coal permeability stress sensitivity

By inserting the corresponding effective stress and coal permeability values into Eqs. (5) and (6), coal *PDR* and α_k at different temperatures are calculated, as illustrated in Fig. 5. With increasing effective stress, *PDR* increases, but α_k decreases. When the range of effective stress is 2.0–4.0 MPa, *PDR* increases rapidly, and α_k decreases sharply. After coal sample effective stress increases to more than 4.0 MPa, the overall trends of increasing *PDR* and decreasing α_k become more moderate. Table 4 represents the specific stress sensitivity evaluation parameters of the coal samples under different temperatures.

According to Table 4, under five temperatures, when effective stress increases from 2.0 to 4.0 MPa, the *PDR* range is 93.87%–96.77%, with a mean of 95.18%. The range of average α_k is 0.1223–0.1238 MPa^{-1}, with a mean of 0.1229 MPa^{-1}. With increasing temperature, *PDR* and average α_T first decrease and then increase, with the minimum value at a temperature of 45°C.

The dimensionless effective stress and permeability are fitted by Eq. (8), which are represented in Table 5. The

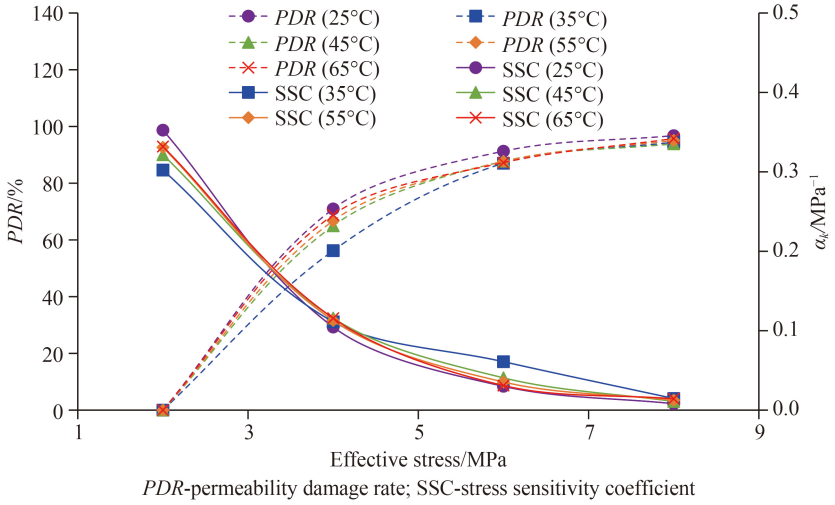

Fig. 5 Relationship between permeability damage rate (*PDR*), stress sensitivity coefficient (SSC) α_k, and effective stress at different temperatures.

Table 4 Stress sensitivity evaluation parameters at different temperatures

Temperature/°C	*PDR*/%	α_k/(MPa^{-1})		
		Maximum	Minimum	Average
25	96.771	0.353	0.008	0.1238
35	94.450	0.302	0.015	0.1223
45	93.871	0.322	0.011	0.1223
55	95.072	0.331	0.013	0.1229
65	95.751	0.332	0.014	0.1232
Average	95.183	0.328	0.012	0.1229
Maximum	96.771	0.353	0.015	0.1238
Minimum	93.871	0.302	0.008	0.1223

Table 5 Statistic results for the new stress sensitivity index *S* of coal samples

Temperature/°C	Fitting formula	*S*	R^2
25	$y = 1.0039x^{-1.976}$	1.976 ± 0. 175	0.995
35	$y = 1.0134x^{-1.546}$	1.546 ± 0.267	0.972
45	$y = 1.0057x^{-1.714}$	1.714 ± 0.156	0.993
55	$y = 1.0049x^{-1.769}$	1.769 ± 0.150	0.994
65	$y = 1.0037x^{-1.821}$	1.821 ± 0.131	0.996

Notes: $x = \sigma/\sigma_0$; $y = k/k_0$.

fitted results show a high correlation (>0.99). From Table 5, under different temperature conditions, the range of stress sensitivity index *S* is 1.546–1.976, with a mean of 1.765. The *S* variation trend with increasing temperature is similar to *PDR* and average α_T.

4.2.2 Analysis of coal permeability temperature sensitivity

Based on Eqs. (5) and (9), it is possible to calculate *PDR* and α_T under different effective stresses (see Fig. 6). As can be seen, with increasing temperature, *PDR* increases, but α_T decreases and exhibits fluctuations. The low-volatile bituminous coal becomes significantly sensitive to temperature at a range of 25°C–45°C; further, its α_T decreases sharply, and its *PDR* increases rapidly. The temperature sensitivity becomes weaker when the temperature exceeds 45°C, and the overall trends of a decreasing α_T and increasing *PDR* become more moderate. The temperature sensitivity evaluation parameters of the coal samples under different stresses are represented in Table 6.

From Table 6, when the sample temperature increases from 25°C to 65°C, the range of *PDR* is 66.667%–89.873%, with a mean of 77.833%, and the range of average α_T is 0.017°C^{-1}–0.020°C^{-1}, with a mean of 0.018°C^{-1}. With increasing effective stress, *PDR* and average α_T first increase, then decrease, and then increase again, reaching maxima at an effective stress of 4.0 MPa.

Equation (10) is used to fit the dimensionless permeability and temperature, which are represented in Table 7. Under different effective stress conditions, the range of temperature sensitivity index S_T is 1.155–2.314, with a mean value of 1.165; the maximum is reached when the effective stress is 4.0 MPa.

The relationship between the stress sensitivity and temperature sensitivity evaluation parameters is shown in Fig. 7. The new sensitivity parameters (*S* and S_T) strongly linearly correlate to the sensitivity regression coefficient (a_1 and a_2) and correlate relatively weakly to *PDR* and the average sensitivity coefficient (α_k and α_T). This is because *PDR*, α_k and α_T reflect the sensitivity of the coal reservoir to stress and temperature over different ranges. The *S* and S_T parameters can provide equivalent information to a_1 and a_2, which can be fitted by experimental results. As evaluation parameters, *S*, S_T, a_1, and a_2 have the advantage that they are unaffected by the number of experimental data points or the temperature

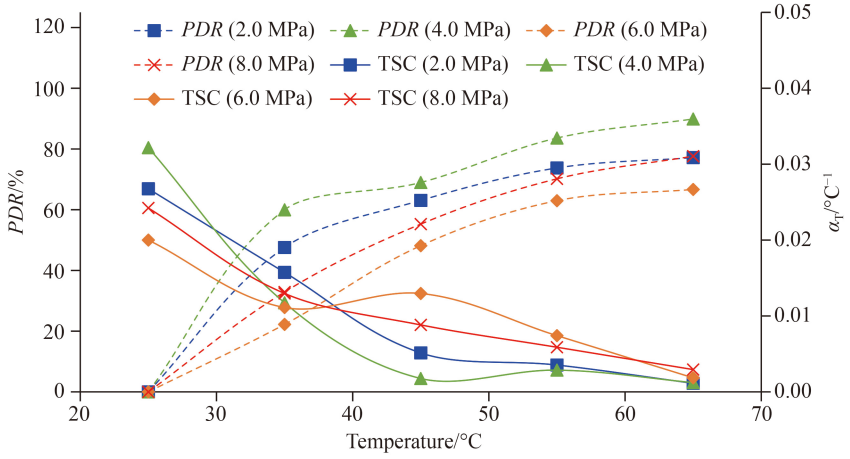

Fig. 6 Relationship between permeability damage rate (*PDR*), temperature sensitivity coefficient (TSC) α_T, and temperature under different effective stresses.

Table 6 Temperature sensitivity evaluation parameters at different effective stresses

Effective stress/MPa	*PDR*/%	α_T/°C^{-1}		
		Maximum	Minimum	Average
2.0	77.163	0.067	0.001	0.018
4.0	89.873	0.080	0.001	0.020
6.0	66.667	0.050	0.002	0.017
8.0	77.627	0.061	0.003	0.018
Average	77.833	0.065	0.002	0.018
Maximum	89.873	0.080	0.003	0.020
Minimum	66.667	0.050	0.001	0.017

and stress conditions. They exhibit both integrality and uniqueness, which can be used to represent the sensitivity of coal reservoir permeability to stress and temperature under certain conditions.

4.3 Coupled influences of stress and temperature on coal permeability

According to experimental results, the permeability variation of the coal samples under the coupled impact of effective stress and temperature is shown in Fig. 8(a). The correlation between the three variables is revealed through the Pearson correlation coefficient method (Fig. 8(b)). The effective stress and temperature together make coal sample permeability decrease in a complex, non-linear manner (Fig. 8(a)). In addition, the calculated degree of correlation coefficient between effective stress and permeability is −0.70, while that between temperature and permeability is −0.22. These results indicate that the impact of effective stress would be more significant than that of temperature on coal permeability.

According to the least square method, the seepage experimental results are regressed. A regression model

Table 7 Statistical results for the new temperature sensitivity index S_T of coal samples

Effective stress/MPa	Fitting formula	S_T	R^2
2.0	$y = 0.9874x^{-1.686}$	1.686 ± 0.09	0.991
4.0	$y = 0.9897x^{-2.314}$	2.314 ± 0.19	0.984
6.0	$y = 1.0307x^{-1.155}$	1.155 ± 0.12	0.962
8.0	$y = 0.9999x^{-1.457}$	1.457 ± 0.10	0.986

Note: $x = T/T_0$; $y = k/k_{0r}$.

among coal permeability k, temperature T, and effective stress σ_e is established:

$$k = \exp(1.0489 - 0.032T - 0.616\sigma_e). \quad (11)$$

To validate this coupled model applicability, a correlation analysis between the measured permeability and its predicted value is carried out, and the square of the correlation coefficient is found to be 0.916, as shown in Fig. 9. In addition, the F function is used to test the effectiveness of the established linear regression equation. The confidence level is taken as $a = 0.01$, the number of independent variables is $n = 2$, and the number of samples is 25. The critical value of the F function under the above conditions, F_a (2, 25), can be obtained by consulting the F function distribution table, which is found to be 5.719. The F statistic of Eq. (11) is 224.93, which is far more than the critical value, and the significance level of the linear regression data are 2×10^{-15} (<0.01). Therefore, Eq. (11) can be used to predict the permeability evolution of medium-rank coal seams at different burial depths.

4.4 Mechanism of coupled effect of temperature and stress on coal reservoir permeability

Coal is composed of natural fractures (cleats) as well as matrix pores. Coal matrix would generally be separated by natural fracture networks, providing migration

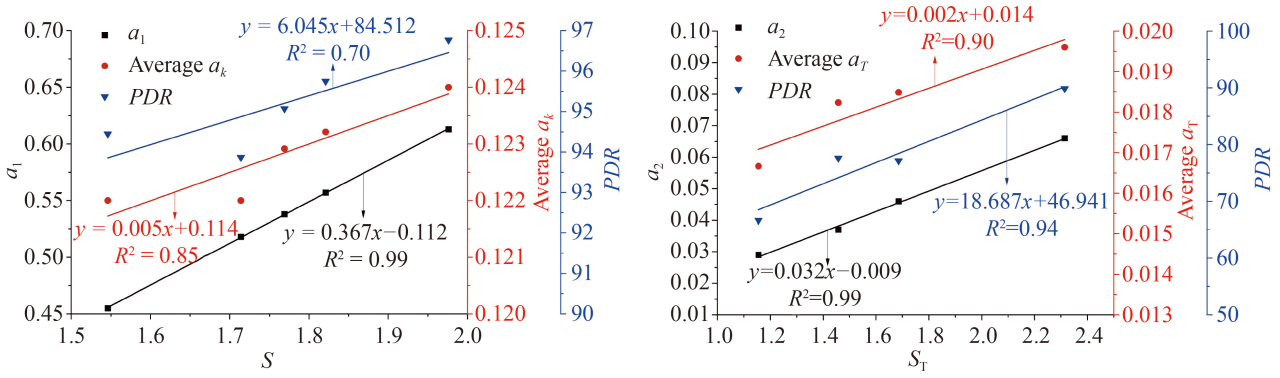

Fig. 7 (a) Correlation analysis of stress sensitivity evaluation parameters. (b) Correlation analysis of temperature sensitivity evaluation parameters.

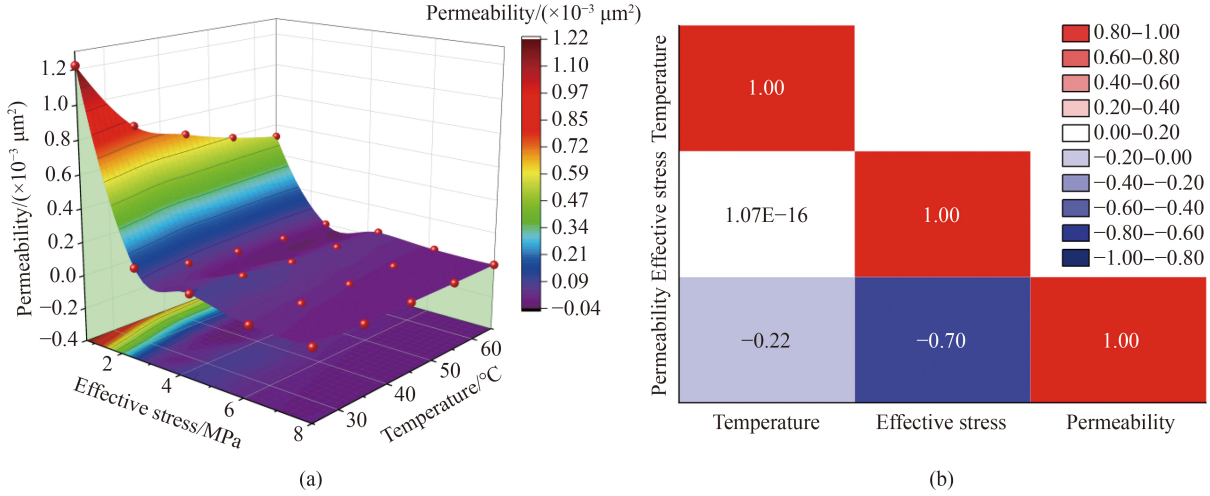

Fig. 8 (a) Coal permeability evolution under the coupled impact of effective stress and temperature; (b) Pearson correlation analysis.

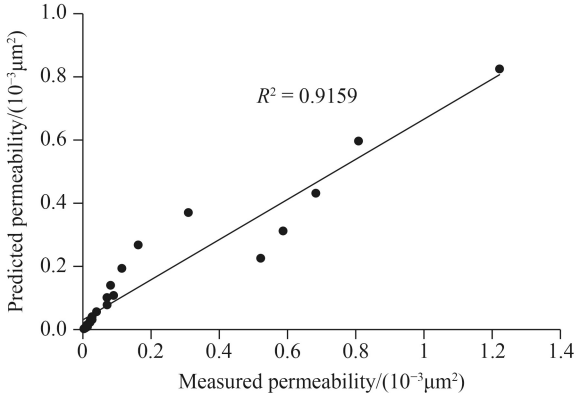

Fig. 9 Comparison between measured and predicted permeability.

channels for free gas and controlling coal permeability (Zhang et al., 2009; Shi et al., 2014). Generally, there is a high density of fractures in coal reservoirs, which is very important for CBM production because not only do the fractures provide storage space, but they are also staggered to form a network system, which connects matrix pores and provides flow channels for the free gas.

As illustrated schematically in Fig. 10, coal reservoirs are generally separated by two groups of mutually perpendicular cleats (Meng et al., 2021). Coal permeability variation with changes in aperture for two such orthogonal sets of fractures can be calculated by the following equation (Zhang et al., 2007):

$$k_z = k_{0x}\left(1-\frac{\Delta b_x}{b_{0x}}\right)^3 + k_{0y}\left(1-\frac{\Delta b_y}{b_{0y}}\right)^3, \qquad (12)$$

where k_z is the variation in coal permeability in the z direction due to aperture increments in the x direction (Δb_x) and y direction (Δb_y), with compressive displacements being positive and tensile displacements being negative; k_{0x} and k_{0y} are the original permeabilities in the x and y directions at initial state, respectively; and b_{0x} and b_{0y} are the average initial normal apertures of fractures in the x and y directions, respectively. From Eq. (12), the permeability of a coal reservoir would be affected by a change in fracture aperture, Δb, which is equal to the initial fracture aperture, b_0, minus the deformed fracture

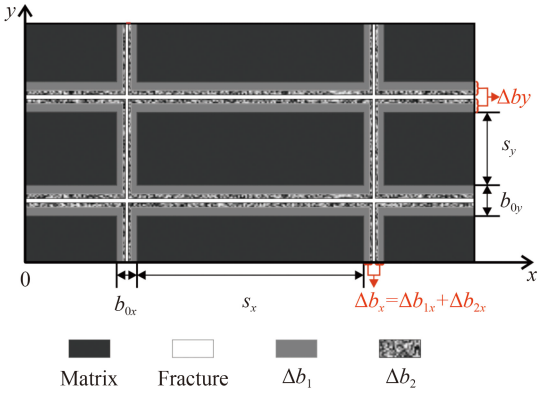

Fig. 10 Simplified multiple fracture system of two groups of orthogonal fracture systems parallel to the *z* direction.

aperture, *b*. The main factors affecting the aperture of coal reservoir fractures are the effective stress and temperature.

The variation in fracture aperture, Δb (mm), can be decomposed as follows:

$$\Delta b = \Delta b_1 + \Delta b_2, \tag{13}$$

where Δb_1 (mm) is the variation in aperture induced by changes in effective stress, and Δb_2 is the variation induced by changes in temperature.

In Eq. (12), the aperture changes of the two groups of fractures in the *x* and *y* directions are $\Delta b_x = b_{0x} - b_x = \Delta b_{1x} + \Delta b_{2x}$ and $\Delta b_y = b_{0y} - b_y = \Delta b_{1y} + \Delta b_{2y}$. The coal reservoir permeability of the two fracture groups can be calculated by substituting Δb_x and Δb_y into Eq. (12).

Our results indicate that coal permeability exhibits significant temperature sensitivity, with increasing temperature, coal reservoir permeability decreases. Generally, the impact of temperature on coal reservoir permeability is manifested in both inhibition and enhancement. It has been shown that the weight-loss rates of coal change notably when the temperature is approximately 100°C or 470°C (Akbarzadeh and Chalaturnyk, 2014). When the temperature exceeds a certain critical temperature, the internal structure of coal changes significantly, and thermal cracking may occur (Niu et al., 2014). Increasing temperature causes coal permeability to decrease continuously below the critical temperature, owing to thermal expansion of the coal matrix. A rising temperature would cause coal reservoir permeability to increase sharply above the critical temperature, which can be attributed to thermal cracking of the coal (Shang et al., 2019). In the Qinshui Basin, the coal reservoir buried depth is mainly above 2000 m, and the temperature is generally lower than 70°C. Within the experimental temperature range, the effect of thermal cracking of the coal on its permeability can be ignored. Therefore, the main cause of the continuous decrease in coal permeability is that temperature rise induces coal matrix expansion induced by the increasing temperature, which would reduce the aperture of coal fractures. Coal matrix thermal expansion strain can be obtained by the following equation:

$$\Delta\varepsilon_{\mathrm{T}} = \alpha_{\mathrm{T}}\Delta T, \tag{14}$$

where $\Delta\varepsilon_{\mathrm{T}}$ is the volumetric strain produced by temperature change, α_{T} is the thermal expansion coefficient, and ΔT (°C) is the variation in temperature. For the same temperature increment, the greater the value of α_{T}, the larger the coal matrix expansion strain will be.

Based on elasticity theory, when an elastomer's temperature changes, each part of it will tend to expand or contract with increasing or decreasing temperature. However, owing to external constraints and mutual constraints between various parts of the elastomer, this expansion or contraction cannot occur freely, and this results in stress (i.e., thermal stress). The expression for the thermal stress $\Delta\sigma_{\mathrm{T}}$ (MPa) is as follows:

$$\Delta\sigma_{\mathrm{T}} = E\Delta\varepsilon_{\mathrm{T}} = E\alpha_{\mathrm{T}}\Delta T, \tag{15}$$

where *E* (MPa) is the elastic modulus of coal.

According to the negative exponential relationship between fracture aperture and stress in coal, when there are two groups of fractures, coal reservoir permeability can be calculated by the following equation (Meng et al., 2011):

$$K_z = K_{0x}\exp\left[-\frac{3(\Delta\sigma_{nx} - \Delta p + \Delta\sigma_{\mathrm{T}x})}{b_{0x}K_{nx}}\right] + K_{0y}\exp\left[-\frac{3\left(\Delta\sigma_{ny} - \Delta p + \Delta\sigma_{\mathrm{T}y}\right)}{b_{0y}K_{ny}}\right], \tag{16}$$

where $\Delta\sigma_{nx} = \sigma_{nx} - \sigma_{nx}^0$ and $\Delta\sigma_{ny} = \sigma_{ny} - \sigma_{ny}^0$ are normal stress variations in the *x* and *y* directions, σ_{nx}^0 and σ_{ny}^0 are the initial normal stress in the *x* and y directions, $\Delta p = p - p_0$ is the pore pressure variation, p_0 is the initial pore pressure, $\Delta\sigma_{\mathrm{T}x} = \sigma_{\mathrm{T}x} - \sigma_{\mathrm{T}x}^0$ and $\Delta\sigma_{\mathrm{T}y} = \sigma_{\mathrm{T}y} - \sigma_{\mathrm{T}y}^0$ are changes in thermal stress in the *x* and *y* directions, $\sigma_{\mathrm{T}x}^0$ and $\sigma_{\mathrm{T}y}^0$ are the initial thermal stress in the *x* and y directions, and K_{nx} and K_{ny} are the normal stiffnesses of the cleats in the *x* and *y* directions.

Assuming coal matrix thermal expansion is isotropic, the thermal stress that it causes can be expressed as

$$\sigma_{\mathrm{T}x} = \sigma_{\mathrm{T}y} = E\alpha_{\mathrm{T}}\Delta T. \tag{17}$$

Combining Eqs. (16) and (17), when considering the coupled impact of temperature and stress, the coal permeability model can be expressed as

$$K_z = K_{0x}\exp\left[-\frac{3(\Delta\sigma_{nx} - \Delta p + E\alpha_{\mathrm{T}}\Delta T)}{b_{0x}k_{nx}}\right] + K_{0y}\exp\left[-\frac{3\left(\Delta\sigma_{ny} - \Delta p + E\alpha_{\mathrm{T}}\Delta T\right)}{b_{0y}k_{ny}}\right]. \tag{18}$$

According to Eq. (18), fractured coal permeability is

impacted by changes in temperature, in addition to being influenced by normal stress and pore pressure. The effect of temperature is consistent with that of the normal stress and in contrast to that of the pore pressure. When the normal stress or temperature increases, coal permeability decreases as a negative exponential function.

5 Conclusions

1) The permeability of the coal samples shows significant sensitivity to stress and temperature. At 25°C, 35°C, 45°C, 55°C, and 65°C, with increasing effective stress, coal sample permeability declines continuously. In the low-stress stage, this decrease is sharp. With further increases in stress, the decrease in permeability gradually slows down. Additionally, under effective stress conditions of 2.0, 4.0, 6.0, and 8.0 MPa, an increase in temperature causes the permeability to decrease continuously, with the rate of decrease becoming less at higher temperatures.

2) A stress sensitivity index S and temperature sensitivity index S_T have been proposed as new stress and temperature sensitivity evaluation parameters. They strongly linearly correlate to the sensitivity regression coefficients (a_1 and a_2), while they correlate relatively weakly to *PDR* and the average sensitivity coefficient (α_k and α_T), which indicates that S, S_T, a_1, and a_2 can be used to represent the sensitivity of coal reservoir permeability to stress and temperature under certain conditions, while *PDR*, α_k, and α_T can be used to characterize the phased stress and temperature sensitivity in with stress and temperature change.

3) As effective stress and temperature increase, the *PDR* of a coal sample increases, while α_k and α_T decrease. With increasing temperature, coal stress sensitivity index S first declines and then rises, with a minimum value at 45°C. Additionally, with increasing effective stress, coal temperature sensitivity index S_T fluctuates, reaching a maximum under an effective stress of 4.0 MPa.

4) A correlation among coal permeability, effective stress, and temperature is revealed through the Pearson correlation coefficient. The correlation between effective stress and permeability is −0.70, while correlation between temperature and permeability is −0.22. This implies that the impact of effective stress on coal reservoir permeability is more serious than temperature.

5) With increasing fracture aperture, coal reservoir permeability increases, which obeys a cubic law. The aperture of coal would be significantly impacted by effective stress and temperature variation. From our derivation, it is believed that coal permeability will exponentially decrease as effective stress and temperature increase.

Acknowledgments This work was financially supported by the National Natural Science Foundation of China (Grant No. 42172190) and the Shanxi Province Science and Technology Major Project (Nos. 20201102001, 20191102001, and 20181101013). The authors thank the reviewers and the editor for their constructive comments.

References

Akbarzadeh H, Chalaturnyk R J (2014). Structural changes in coal at elevated temperature pertinent to underground coal gasification: a review. Int J Coal Geol, 131: 126–146

Bear J, Corapcioglu M Y (1981). A mathematical model for consolidation in thermoelastic aquifer due to hot water injection or pumping. Water Resour Res, 17(3): 723–736

Biot M A (1954). Theory of elasticity and consolidation for a porous anisotropic solid. J Appl Phys, 26(2): 182–185

Chu T X, Yu M G, Jiang D Y (2016). Experimental investigation on the permeability evolution of compacted broken coal. Transp Porous Media, 116(2): 1–22

Durucan S, Edwards J S (1986). The effects of stress and fracturing on permeability of coal. Min Sci Technol, 3(3): 205–216

Gao Z, Li B B, Li J H, Wang B, Ren C H, Xu J, Chen S (2021). Coal permeability related to matrix-fracture interaction at different temperatures and stresses. J Petrol Sci Eng, 200: 108428

Jones F O, Owens W W (1980). A laboratory study of low-permeability gas sands. J Pet Technol, 32(9): 1631–1640

Karthikeyan, G., Chand, J., Chatterjee, R., (2020). Impact of geomechanics in coal bed methane development and production, barakar coals in central India. J Pet Sci Eng, 194(1): 107515.

Li Z Q, Xian X F, Long Q M (2009). Experiment study of coal permeability under different temperature and stress. J China Univ Min Technol, 38: 523−527 (in Chinese)

Liu Q S, Liu X W (2014). Research on critical problem for fracture network propagation and evolution with multifield coupling of fractured rock mass. Rock and Soil Mechanics 35(2): 305−320 (in Chinese)

Liu T, Lin B Q, Yang W (2017). Impact of matrix–fracture interactions on coal permeability: model development and analysis. Fuel, 207: 522–532

McKee C R, Bumb A C, Koenig R A (1998). Stress-dependent permeability and porosity of coal. Rocky Mt Assoc Geol: 143–153

Meng Y, Li Z P, Lai F P (2021). Influence of effective stress on gas slippage effect of different rank coals. Fuel, 285: 119207

Meng Y, Wang J Y, Li Z P, Zhang J X (2018). An improved productivity model in coal reservoir and its application during coalbed methane production. J Nat Gas Sci Eng, 49: 342–351

Meng Z P, Li G Q (2013). Experimental research on the permeability of high-rank coal under a varying stress and its influencing factors. Eng Geol, 162: 108–117

Meng Z P, Liu S M (2018). Geology and Engineering of Coalbed Methane Development in Coal Mine Area. Beijing: Science Press

Meng Z P, Zhang J X, Liu H, Liu S S, Zhou X D (2014). Productivity model of CBM wells considering the stress sensitivity and its application analysis. J China Coal Soc, 39(04): 593−599 (in Chinese)

Meng Z P, Zhang J C, Wang R (2011). *In-situ* stress, pore pressure and

stress-dependent permeability in the Southern Qinshui Basin. Int J Rock Mech Min Sci, 48(1): 122–131

Niu S W, Zhao Y S, Hu Y Q (2014). Experimental investigation of the temperature and pore pressure effect on permeability of lignite under the *in-situ* condition. Transp Porous Media, 101(1): 137–148

Norishad J (1989). Coupled thermal–hydraulic–mechanical phenomena in saturated fractured porous rocks: numerical approach. J Geophys Res, 89(B12): 10365–10373

Oda M (1985). Permeability tensor for discontinuous rock masses. Geotechnique, 5(4): 483–495

Ohnishi Y, Ohtsu H, Nakamura I (1982). Coupled stress-flow finite element analysis of rock slope near pressure tunnel. In: International Committee for Numerical Methods in Geomechanics. Vol. 2: 579–585. Canadian Geotechnical Society, Edmonton: Alberta

Pan Z J, Connell L D (2012). Modelling permeability for coal reservoirs: a review of analytical models and testing data. Int J Coal Geol, 92: 1–44

Perera M (2017). Influences of CO_2 injection into deep coal seams: a review. Energy Fuels, 31(10): 10324–10334

Sakurovs R, Day S, Weir S, Duffy G (2008). Temperature dependence of sorption of gases by coals and charcoals. Int J Coal Geol, 73(3–4): 250–258

Shang X J, Wang J G, Zhang Z Z, Gao F (2019). Three-parameter permeability model for the cracking process of fractured rocks under temperature change and external loading. Int J Rock Mech Min Sci, 123: 104106

Shi J Q, Durucan S (2005). A model for changes in coalbed permeability during primary and enhanced methane recovery. SPE Reservoir Eval Eng, 8(4): 291–299

Shi J Q, Durucan S, Shimada S (2014). How gas adsorption and swelling affects permeability of coal: a new modelling approach for analysing laboratory test data. Int J Coal Geol, 128−129: 134−142

Somerton W H, Soylemezoglu M, Dudley R C (1975). Effect of stress on permeability of coal. Int J Rock Mech Min Sci Geomech Abstr, 12(5–6): 129–145

Sparks D P, Mclendon T H, Saulsberry J L, Lambert S W (1995). The effects of stress on coalbed reservoir performance, Black Warrior Basin, USA. In: Proc. 1995 SPE Annual Technical Conference and Exhibition, Paper SPE 30743, Dallas, Texas

Teng T, Wang J G, Gao F, Ju Y, Jiang C B (2016). A thermally sensitive permeability model for coal-gas interactions including thermal fracturing and volatilization. J Nat Gas Sci Eng, 32: 319–333

Terzaghi K (1943). Theoretical Soil Mechanics. New York: Wiley

Wang J M, Zhao Y S, Mao R B (2019). Impact of temperature and pressure on the characteristics of two-phase flow in coal. Fuel, 253: 1325–1332

Yin G Z, Jiang C B, Wang J G, Xu J (2013). Combined effect of stress, pore pressure and temperature on methane permeability in anthracite coal: an experimental study. Transp Porous Media, 100(1): 1–16

Zhang J, Standifird W B, Roegiers J C, Zhang Y (2007). Stress-dependent fluid flow and permeability in fractured media: from Lab experiments to engineering applications. Rock Mech Rock Eng, 40(1): 3–21

Zhang J, Lang J, Standifird W. (2009). Stress, porosity, and failure-dependent compressional and shear velocity ratio and its application to wellbore stability. J Pet Sci Eng, 69(3–4): 193–202